

Mechanism of Nitric Oxide Oxidation Reaction ($2\text{NO} + \text{O}_2 \rightarrow 2\text{NO}_2$) Revisited

Oleg B. Gadzhiev,^{*,†,‡} Stanislav K. Ignatov,[†] Shruba Gangopadhyay,[§] Artëm E. Masunov,[§] and Alexander I. Petrov^{||}

[†]Department of Chemistry, N.I. Lobachevsky State University of Nizhny Novgorod, 23 Gagarin Avenue, Nizhny Novgorod 603950, Russia

[‡]Institute of Applied Physics of the Russian Academy of Sciences, 46 Ul'yanov Street 603950, Nizhny Novgorod, Russia

[§]NanoScience Technology Center, Department of Chemistry and Department of Physics, University of Central Florida, 12424 Research Parkway, Ste 400, Orlando, Florida 32826, United States

^{||}Department of Metallurgy of Noble and Rare Metals, Institute of Non-Ferrous Metals and Materials Science, Siberian Federal University, 81 Svobodny Prospect, Krasnoyarsk 660041, Russia

 Supporting Information

ABSTRACT: The reaction between molecular oxygen and two nitric oxide(II) molecules is studied with high-level *ab initio* wave function methods, including geometry optimizations with coupled cluster (CCSD(T_{full})/cc-pCVTZ) and complete active space with second order perturbation theory levels (CASPT2/cc-pVDZ). The energy at the critical points was refined by calculations at the CCSD(T_{full})/aug-cc-pCVTZ level. The controversies found in the previous theoretical studies are critically discussed and resolved. The best estimate of the activation energy is 6.47 kJ/mol.

This work is focused on the elucidation of the thermal reaction mechanism between dioxygen and two nitrogen monoxide molecules. Very recently, comprehensive experimental^{1,2} and joined quantum chemical and experimental³ investigations were performed for NO/O₂ and related (NO/O₂[•]) systems.⁴ The formal kinetics of third order reactions are in the scope of current theoretical developments.⁵ Measurements of the rate constant and activation energy of the reaction $2\text{NO} + \text{O}_2$ were reviewed in ref 6, which covered the years up to the early 1990s. The most recent investigation, which was not included in ref 6, is ref 1. The most reliable value of activation energy determined up to date⁷ is $-4.41 [\pm 3.33]$ kJ/mol in the temperature range 270–600 K (see also ref 8).

The mechanism we report here was found to be different from the mechanisms studied previously by Olson et al.⁹ and other authors.¹⁰ This Letter supports the mechanism proposed by McKee.¹¹ The classical Eyring–Gershinowitz mechanism¹² was studied in more detail by McKee,¹¹ who used *ab initio* and DFT (B3LYP) methods. However, the geometries of intermediates and transitions states for the two-step mechanism¹¹ must be refined, and physicochemical parameters of the elementary reactions must be revisited using recent developments in the coupled cluster method.¹³

In ref 11, transition states were not optimized uniformly. In the present report, we will show the two-step mechanism of the reaction $2\text{NO} + \text{O}_2 \rightarrow 2\text{NO}_2$ using the CCSD(T) and CASSCF methods with full geometry optimizations.

Recently, we investigated¹⁰ the potential energy surfaces (PES) of the $2\text{NO}_2 + \text{O}_2$ system using broken symmetry DFT (BS-UDFT), double hybrid DFT, and CCSD(T)//DFT approaches. In the study,¹⁰ we found perfect agreement between

the recommended experimental activation energy^{6,7} and calculated (B3LYP/*aug-pc3*) activation enthalpy (Tables 1, 6, and 7 and Figure 6 in ref 3) when the reaction proceeded via the cyclic intermediate CC–INT (Scheme 1).

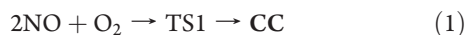
However, the wave function of this system was found to be multiconfigurational, as evidenced by the high values for the T₁ test within the CCSD method. In this Letter, we reinvestigate the PES using CASSCF, CASPT2, and MRMP2 methods that are more appropriate for describing the multiconfigurational character of the CC–INT ground state.

Complete geometry optimization of the stationary points on PES is performed at the RCCSD(T)/cc-pVDZ and UCCSD(T)/cc-pVDZ levels (using the GAMESS-US¹⁴ and Gaussian 2003¹⁵ codes, respectively). Numerical calculations of the force constant matrix were performed to verify the types of stationary points. The intrinsic reaction coordinate (IRC) was identified for all of the transition states. The T₁-test values were below 0.036 for all of the optimized geometries. The structure and relative energies of several stationary points including CC–INT were found to differ from earlier BS-UDFT results.¹⁰ The valley–pitchfork bifurcation point in the main reaction channel, reported previously,¹⁰ was not found here. The elementary steps reported in Figure 1 and in the Supporting Information are as follows (the relative energies at the CCSD(T)/cc-pVDZ theory level are in parentheses): $2\text{NO} + \text{O}_2$ (0 kJ/mol) \rightarrow TS1 (13.98 kJ/mol) \rightarrow CC (–16.41 kJ/mol) \rightarrow TS2 (1.62 kJ/mol) \rightarrow 2NO_2 (–73.95 kJ/mol).

Received: December 29, 2010

Published: May 30, 2011

In contrast to the results reported in refs 9 and 10, the mechanism presented here (see Figure 1) takes place entirely on the singlet state potential surface and consists of two steps:



The initial step (1) is the formation of the CC intermediate with the saddle point TS1 and an activation barrier of 13.98 kJ/mol (in refs 9 and 10, this was barrierless elementary reaction $2\text{NO} + \text{O}_2 \rightarrow \text{CC}$). The second step (2) with the saddle point TS2 corresponds to the homolysis of CC (in refs 9 and 10, conformer CC rearranged in CC–INT, which was involved in the main multistep reaction channel, $\text{CC} \rightarrow \text{CC} \rightarrow \text{INT} \rightarrow \text{cis-ONONO}_2 \rightarrow \text{trans-ONONO}_2 \rightarrow \text{O}_2\text{NNO}_2 \rightarrow 2\text{NO}_2$). Elementary reaction 1 (3) is the rate-determining step of the proposed mechanism (in refs 9 and 10, isomerization $\text{CC} \rightarrow \text{CC} \rightarrow \text{INT}$ was the rate-determining step).

To verify the results at the CCSD(T)/cc-pVDZ theory level, the fragments of a potential energy surface corresponding to reactions 1 and 2 have been calculated at the levels CASSCF(10,10)/cc-pVDZ (Gaussian 03) and CASSCF(10,10)/cc-pVTZ (GAMESS-US). These calculations confirm the transition state TS1 (CAS(10,10)/cc-pVDZ) during the formation of the complex CC (CAS(10,10) with cc-pVDZ and cc-pVTZ basis

sets) in the initial step through the intrinsic reaction coordinate (IRC) method at the CAS(10,10)/cc-pVDZ level starting from TS1 in both directions. For reaction 2, localization of TS2 in the CASSCF method was complicated by the intruder states. The analysis of the configuration interaction (CI) amplitudes for CASSCF(10,10)/cc-pVDZ (obtained in this paper for both intermediate CC and TS1) and CASSCF(10,12)/cc-pVDZ (only for CC) and CAS(26,16)/cc-pVDZ (given earlier for CC–INT and O_2NNO_2)³ shows that the relative weight of the Hartree–Fock configuration (the square of the first coefficient in the CI expansion vector) is greater than 0.8 for all stationary points except CC–INT (CAS(26,16)) and TS1 (CAS(10,10)). This allows us to conclude that the errors of a single-reference CCSD(T) approximation do not influence the results significantly. We consider the CCSD(T) method more reliable than CASSCF since it takes into account the dynamic electron correlation.

To eliminate the contradiction¹⁰ between KS-DFT, BS-UDFT, and CASSCF on the structure of the intermediate CC–INT, the complete optimization of its geometry at the levels CCSD(T)/cc-pVDZ and CAS(2,2)PT2/cc-pVDZ (using MOLPRO software¹⁶) and MR(2,2)MP2/cc-pVDZ (using GAMESS-US software) has been carried out. A good agreement between the optimized geometric parameters has been achieved; the optimized geometries are shown in Figure 2. This allows us to make a conclusion about the reliability of the CCSD(T) results.

Scheme 1. Structure of the Planar Cyclic Intermediate CC–INT (a) from Previous Investigations^{9,10} and Structures of TS1 (b), CC (c), and TS2 (d) of the Reaction Path from the Presented Letter (See Text for Details)

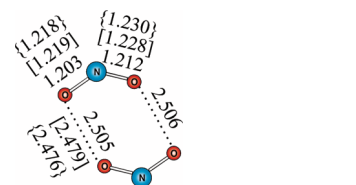
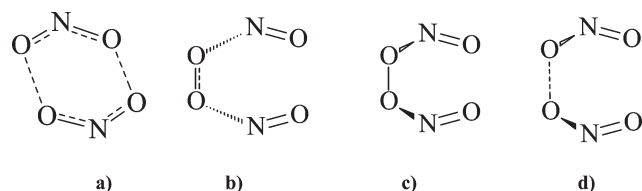


Figure 2. Geometries of intermediate CC–INT optimized at the levels CCSD(T)/cc-pVDZ, CASPT2/cc-pVDZ [square brackets], and MRMP2/cc-pVDZ {curly brackets}. Bond lengths are indicated in Ångstroms.

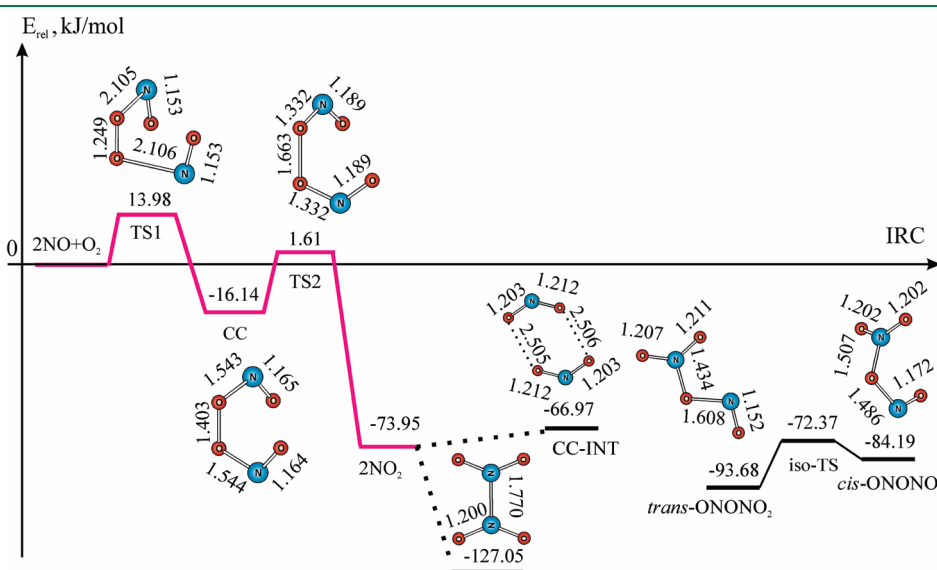


Figure 1. Profile of singlet PES of thermal reaction $2\text{NO}_2 + \text{O}_2 \rightarrow 2\text{NO}_2$, obtained at the CCSD(T)/cc-pVDZ level in the present study. The solid and dotted lines indicate the minimum energy pathways at the CCSD(T)/cc-pVDZ and CAS(26,16)/cc-pVDZ levels, respectively. Bond lengths are indicated in Ångstroms; the relative energies are in kilojoules per mole.

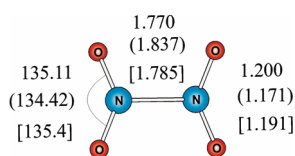


Figure 3. Geometries of dinitrogen tetroxide O_2NNO_2 optimized at the CCSD(T)/cc-pVDZ and CASSCF/cc-pVDZ (parentheses) levels and experimental data¹⁸ [square brackets]. Bond lengths are indicated in Ångströms; the bond angle is in degrees.

This also proves that the previous¹⁰ KS-DFT results are invalid. The isomerization paths $\text{CC} \rightarrow \text{CC-INT}$ and $\text{CC-INT} \rightarrow \text{cis-ONONO}_2$ proposed previously^{9,10} and $\text{CC-INT} \rightarrow \text{trans-ONONO}_2$ were not found at any levels of CCSD(T) or CASSCF employed in the presented investigation. However, the isomerization reaction $\text{cis-ONONO}_2 \rightarrow \text{iso-TS} \rightarrow \text{trans-ONONO}_2$ was reproduced by calculations at the CAS(26,16)/cc-pVDZ and CCSD(T)/cc-pVDZ levels (see Figure 1). The dissociation reactions $\text{cis-ONONO}_2 \rightarrow 2\text{NO}_2$ ($E_r = -21.62$ kJ/mol) and $\text{trans-ONONO}_2 \rightarrow 2\text{NO}_2$ ($E_r = 1.85$ kJ/mol) with corresponding TSs were established at the CAS(26,16)/cc-pVDZ level and characterized by activation energies of 1.8 and 71.1 kJ/mol, respectively. We were unable to locate both TSs at the CCSD(T)/cc-pVDZ level despite an extra effort (relaxed scans of O–N bonds and Hessian calculations). We suppose that these differences in the calculation results are due to the different amounts of nondynamical electron correlation accounted for by the CCSD(T) and CASSCF methods. Additional calculations may be necessary for unambiguous determination of MEPs for these two reactions.

The existence of the saddle point TS2 with an energy of +1.62 kJ/mol (see Figure 1) detected at the CCSD(T)/cc-pVDZ theory level points to the possibility that reaction $2\text{NO} + \text{O}_2 \rightarrow 2\text{NO}_2$ takes place without the formation of intermediate CC-INT (which is now a local minimum on the potential energy surface with a relatively high energy of −66.97 kJ/mol).

The energy of the dimerization reaction with $2\text{NO}_2 \rightarrow \text{O}_2\text{NNO}_2$ calculated at the CCSD(T)/cc-pVDZ level (−53.01 and −38.48 kJ/mol corrected by ZPVE) agrees with the experimental enthalpy of −53.60 kJ/mol;¹⁷ the CASSCF/cc-pVDZ energy (−36.4 and −6.6 kJ/mol with ZPVE) is noticeably underestimated even for the large active space CAS(26,16). Calculated geometrical parameters (bond distances $r(\text{N-N}) = 1.770$ Å, $r(\text{N=O}) = 1.200$ Å, and bond angle $\angle(\text{ONO}) = 135.1^\circ$) at the CCSD(T)/cc-pVDZ level shown in Figure 3 are closer to the corresponding experimental¹⁸ data (bond distances $r(\text{N-N}) = 1.782$ Å, $r(\text{N=O}) = 1.191$ Å, and bond angle $\angle(\text{ONO}) = 135.4^\circ$) than to the geometrical parameters optimized at the CAS(26,16)/cc-pVDZ level (bond distances $r(\text{N-N}) = 1.837$ Å, $r(\text{N=O}) = 1.171$ Å, and bond angle $\angle(\text{ONO}) = 134.4^\circ$).

The found activation character of the elementary reaction $2\text{NO} + \text{O}_2 \rightarrow \text{TS1} \rightarrow \text{CC}$ agrees with the weak negative dependence of the reaction ($2\text{NO} + \text{O}_2 \rightarrow 2\text{NO}_2$) rate constant on the temperature if we assume that the positive barrier height is a consequence of the basis set superposition error (BSSE), and the basis set expansion will make it possible to lower E_a to be in quantitative agreement with the apparent activation energy⁷ of about −4.41 kJ/mol.

We performed an additional search of stationary points O_2 , NO , and TS1 at the CCSD(T,*full*)/cc-pCVTZ level and energy

calculations using the compound approach CCSD(T,*full*)/aug-cc-pCVTZ//CCSD(T,*full*)/cc-pCVTZ by means of the CFOUR suite of programs.¹⁹ The addition of diffuse functions to the basis set (augmentation) significantly improved the barrier height of reaction 1 from 20.99 to 6.47 kJ/mol, which is close to the 0 kJ/mol of the classical Eyring–Gershinowitz¹² estimation of activation energy of the reaction ($2\text{NO} + \text{O}_2 \rightarrow 2\text{NO}_2$) using the Bodenstein experimental data.²⁰ This is also in reasonably good agreement with the latest value⁷ of −4.41 [± 3.33] kJ/mol recommended for the temperature range 270–600 K.

The presented results show that a balanced treatment of both dynamic and static electron correlation is necessary for the correct energy estimation of PES stationary points for the $2\text{NO} + \text{O}_2$ system, and application of a coupled-cluster method requires the inclusion of at least triple excitations. To achieve chemical accuracy in order to quantitatively compare physicochemical parameters of the reaction ($2\text{NO} + \text{O}_2 \rightarrow 2\text{NO}_2$), focal-point analysis (with extrapolations) is probably required. On the basis of the results obtained here, we conclude that the CCSD(T) approach, in contrast with DFT theory, supports the two-step mechanism of nitric oxide oxidation.

■ ASSOCIATED CONTENT

S Supporting Information. The calculated Cartesian coordinates, total energies, vibrational frequencies, and IRC curves. This material is available free of charge via the Internet at <http://pubs.acs.org>

■ AUTHOR INFORMATION

Corresponding Author

*E-mail: euriscomail@mail.ru.

■ ACKNOWLEDGMENT

This work was supported in part by the U.S. National Science Foundation (CHE-0832622). O.B.G. is thankful for the partial support of this study provided by a grant from the Government of the Russian Federation under agreement no. 11.G34.31.0014. S.K.I. acknowledges the RFBR project 11-03-00085. A.I.P. is thankful to SFU Supercomputer Centre for a generous donation of CPU time. A.E.M. and S.G. are grateful to DOE NERSC (project m513), I2lab, and Institute for Simulation and Training (IST) for computer time provided.

■ REFERENCES

- (1) Galliker, B.; Kissner, R.; Nauser, T.; Koppenol, W. H. *Chem.—Eur. J.* **2009**, *15*, 6161.
- (2) Beckers, H.; Willner, H.; Jacox, M. E. *ChemPhysChem* **2009**, *10*, 706.
- (3) Beckers, H.; Zeng, X.; Willner, H. *Chem.—Eur. J.* **2010**, *16*, 1506.
- (4) Botti, H.; Möller, M. N.; Steinmann, D.; Nauser, T.; Koppenol, W. H.; Denicola, A.; Radi, R. *J. Phys. Chem. B* **2010**, *114*, 16584.
- (5) Williams, B. J. *Math. Chem.* **2011**, *49*, 328.
- (6) Tsukahara, H.; Ishida, T.; Mayumi, M. *Nitric Oxide: Biol. Ch.* **1999**, *3*, 191.
- (7) Atkinson, R.; Baulch, D. L.; Cox, R. A.; Crowley, J. N.; Hampson, R. F.; Hynes, R. G.; Jenkin, M. E.; Rossi, M. J.; Troe, J. *Atmos. Chem. Phys.* **2004**, *4*, 1461.
- (8) Manion, J. A.; Huie, R. E.; Levin, R. D.; Burgess, D. R., Jr.; Orkin, V. L.; Tsang, W.; McGivern, W. S.; Hudgens, J. W.; Knyazev, V. D.; Atkinson, D. B.; Chai, E.; Tereza, A. M.; Lin, C.-Y.; Allison, T. C.

Mallard, W. G.; Westley, F.; Herron, J. T.; Hampson, R. F.; Frizzell, D. H. NIST Chemical Kinetics Database, NIST Standard Reference Database 17, Version 7.0 (Web Version), Release 1.4.3, Data version 2008.12; National Institute of Standards and Technology, Gaithersburg, MD. Web address: <http://kinetics.nist.gov> (accessed Apr 15, 2011).

(9) Olson, L. P.; Kuwata, K. T.; Bartberger, M. D.; Houk, K. N. *J. Am. Chem. Soc.* **2002**, *124*, 9469.

(10) Gadzhiev, O. B.; Ignatov, S. K.; Razuvaev, A. G.; Masunov, A. E. *J. Phys. Chem. A* **2009**, *113*, 9092.

(11) McKee, M. L. *J. Am. Chem. Soc.* **1995**, *117*, 1629.

(12) Gershinowitz, H.; Eyring, H. *J. Am. Chem. Soc.* **1935**, *57*, 985.

(13) Harding, M. E.; Metzroth, T.; Gauss, J.; Auer, A. A. *J. Chem. Theory Comput.* **2007**, *4*, 64.

(14) Schmidt, M.; Baldrige, K. K.; Boatz, J. A.; Elbert, S.; Gordon, M.; Jensen, J. H.; Koeski, S.; Matsunaga, N.; Nguyen, K. A.; Su, S. J.; Windus, T. L.; Dupuis, M.; Montgomery, J. A. *J. Comput. Chem.* **1993**, *14*, 1347.

(15) Frisch, M. J.; Trucks, G. W.; Schlegel, H. B.; Scuseria, G. E.; Robb, M. A.; Cheeseman, J. R.; Montgomery, J. A., Jr.; Vreven, T.; Kudin, K. N.; Burant, J. C.; Millam, J. M.; Iyengar, S. S.; Tomasi, J.; Barone, V.; Mennucci, B.; Cossi, M.; Scalmani, G.; Rega, N.; Petersson, G. A.; Nakatsuji, H.; Hada, M.; Ehara, M.; Toyota, K.; Fukuda, R.; Hasegawa, J.; Ishida, M.; Nakajima, T.; Honda, Y.; Kitao, O.; Nakai, H.; Klene, M.; Li, X.; Knox, J. E.; Hratchian, H. P.; Cross, J. B.; Bakken, V.; Adamo, C.; Jaramillo, J.; Gomperts, R.; Stratmann, R. E.; Yazyev, O.; Austin, A. J.; Cammi, R.; Pomelli, C.; Ochterski, J. W.; Ayala, P. Y.; Morokuma, K.; Voth, G. A.; Salvador, P.; Dannenberg, J. J.; Zakrzewski, V. G.; Dapprich, S.; Daniels, A. D.; Strain, M. C.; Farkas, O.; Malick, D. K.; Rabuck, A. D.; Raghavachari, K.; Foresman, J. B.; Ortiz, J. V.; Cui, Q.; Baboul, A. G.; Clifford, S.; Cioslowski, J.; Stefanov, B. B.; Liu, G.; Liashenko, A.; Piskorz, P.; Komaromi, I.; Martin, R. L.; Fox, D. J.; Keith, T.; Al-Laham, M. A.; Peng, C. Y.; Nanayakkara, A.; Challacombe, M.; Gill, P. M. W.; Johnson, B.; Chen, W.; Wong, M. W.; Gonzalez, C.; Pople, J. A. *Gaussian 03*, Version D.02; Gaussian, Inc.: Wallingford, CT, 2007.

(16) Werner, H.-J.; Knowles, P. J.; Manby, F. R.; Schütz, M.; Celani, P.; Knizia, G.; Korona, T.; Lindh, R.; Mitrushenkov, A.; Rauhut, G.; Adler, T. B.; Amos, R. D.; Bernhardsson, A.; Berning, A.; Cooper, D. L.; Deegan, M. J. O.; Dobbyn, A. J.; Eckert, F.; Goll, E.; Hampel, C.; Hesselmann, A.; Hetzer, G.; Hrenar, T.; Jansen, G.; Köppl, C.; Liu, Y.; Lloyd, A. W.; Mata, R. A.; May, A. J.; McNicholas, S. J.; Meyer, W.; Mura, M. E.; Nicklass, A.; Palmieri, P.; Pflüger, K.; Pitzer, R.; Reiher, M.; Shiozaki, T.; Stoll, H.; Stone, A. J.; Tarroni, R.; Thorsteinsson, T.; Wang, M.; Wolf, A. *MOLPRO*, version 2009.1; University College Cardiff Consultants: Cardiff, Wales, 2009.

(17) Chase, J. M. W.; Curnutt, J. L.; Downey, J. J. R.; McDonald, R. A.; Syverud, A. N.; Valenzuela, E. A. *J. Phys. Chem. Ref. Data* **1982**, *11*, 695.

(18) McClelland, B. W.; Gundersen, G.; Hedberg, K. *J. Chem. Phys.* **1972**, *56*, 4541.

(19) Stanton, J. F.; Gauss, J.; Harding, M. E.; Szalay, P. G.; Auer, A. A.; Bartlett, R. J.; Benedikt, U.; Berger, C.; Bernholdt, D. E.; Bomble, Y. J.; Cheng, L.; Christiansen, O.; Heckert, M.; Heun, O.; Huber, C.; Jagau, T.-C.; Jonsson, D.; Jusélius, J.; Klein, K.; Lauderdale, W. J.; Matthews, D. A.; Metzroth, T.; O'Neill, D. P.; Price, D. R.; Prochnow, E.; Ruud, K.; Schiffmann, F.; Schwalbach, W.; Stopkowitz, S.; Tajti, A.; Vázquez, J.; Wang, F.; Watts, J. D. *CFOUR*. Integral packages *MOLE-CULE* (Almlöf, J.; Taylor, P. R.), *PROPS* (Taylor, P. R.), *ABACUS* (Helgaker, T.; Jensen, H. J. Aa.; Jørgensen, P.; Olsen, J.), and ECP routines by Mitin, A. V.; van Wüllen, C. For the current version, see <http://www.cfour.de> (accessed Feb 23, 2011).

(20) Bodenstein, M. *Z. Physik. Chem.* **1922**, *100*, 68.